

# *Astragalus* polysaccharides attenuate pulmonary fibrosis by inhibiting the epithelial-mesenchymal transition and NF- $\kappa$ B pathway activation

RUI ZHANG<sup>1</sup>, LIMING XU<sup>2</sup>, XIAOXIA AN<sup>3</sup>, XINBING SUI<sup>4</sup> and SHUANG LIN<sup>5</sup>

<sup>1</sup>Department of Internal Medicine, The Wuyun Mountain Sanatorium of Hangzhou; Departments of <sup>2</sup>Pathology and <sup>3</sup>Anesthesiology, The First Affiliated Hospital, College of Medicine, Zhejiang University; <sup>4</sup>Department of Medical Oncology, Holistic Integrative Oncology Institutes and Holistic Integrative Cancer Center of Traditional Chinese and Western Medicine, The Affiliated Hospital of Hangzhou Normal University, College of Medicine, Hangzhou Normal University;

<sup>5</sup>Department of Thoracic Surgery, The First Affiliated Hospital, College of Medicine, Zhejiang University, Hangzhou, Zhejiang 310000, P.R. China

Received January 27, 2020; Accepted March 17, 2020

DOI: 10.3892/ijmm.2020.4574

**Abstract.** *Astragalus* polysaccharides (APS), the active ingredients isolated from the plant *Astragalus*, have been reported to have numerous biological activities, including anti-inflammatory and antitumor activities. However, the effect of APS on pulmonary fibrosis (PF) remains unknown. The present study aimed to evaluate the protective effect of APS against PF and to explore its underlying mechanisms by using *in vivo* and *in vitro* models. A mouse *in vivo* model of bleomycin-induced PF and an *in vitro* model of transforming growth factor  $\beta$ 1 (TGF- $\beta$ 1)-stimulated human lung epithelial A549 cells were established. Histopathologic examination and collagen deposition were investigated by hematoxylin and eosin staining and Masson staining, and by detecting the hydroxyproline content. The expression of related genes was analyzed by western blotting, reverse transcription-quantitative (RT-q) PCR, immunofluorescence and immunohistochemistry. The results from the *in vivo* mouse model demonstrated that treatment with APS could ameliorate collagen deposition and reduce fibrotic area and hydroxyproline content in the matrix. Furthermore,

APS significantly inhibited the epithelial-mesenchymal transition (EMT), as evidenced by an increased level of E-cadherin and a decreased expression of vimentin and alpha smooth muscle actin. Furthermore, APS treatment significantly decreased TGF- $\beta$ 1-induced EMT and NF- $\kappa$ B pathway activation *in vitro*. The results from the present study provided new insights on PF regression via the anti-fibrotic effects of APS.

## Introduction

Idiopathic pulmonary fibrosis (IPF) is a chronic, progressive, fibrotic interstitial pulmonary disease of unknown cause, characterized primarily by the excessive deposition of extracellular matrix (ECM) proteins by activated lung fibroblasts and myofibroblasts, leading to decreased gas exchange and impaired pulmonary function (1,2). IPF is one of the most common idiopathic interstitial pneumonia and the most common interstitial pulmonary disease, with an estimated incidence of 50/100,000 worldwide every year, with a median survival time after diagnosis of 3-5 years (3,4).

IPF commonly occurs in older adults, and the median survival rate of patients with IPF after diagnosis is very poor (5,6). Previous studies on IPF reported that some anti-fibrinolytic components, glucocorticoids, antioxidants and other therapeutic strategies are effective in the laboratory. However, certain drugs, including glucocorticoids and immunosuppressants, have serious adverse effects and do not improve the prognosis of patients. At present, there is no universally accepted treatment for IPF. Although the new anti-fibrotic drugs pirfenidone and nintedanib can slow down IPF progression, their effectiveness and long-term safety remain controversial (7). It is therefore crucial to determine potential targets in IPF and develop novel treatments for patients.

Although many traditional Chinese herbs (TCH) have interesting therapeutic effects in various types of disease (8,9), only a few TCHs have been reported to have therapeutic effects

---

*Correspondence to:* Dr Shuang Lin, Department of Thoracic Surgery, The First Affiliated Hospital, College of Medicine, Zhejiang University, 79 Qingchun Road, Hangzhou, Zhejiang 310000, P.R. China  
E-mail: shuanglin@zju.edu.cn

Professor Xinbing Sui, Department of Medical Oncology, Holistic Integrative Oncology Institutes and Holistic Integrative Cancer Center of Traditional Chinese and Western Medicine, The Affiliated Hospital of Hangzhou Normal University, College of Medicine, Hangzhou Normal University, 2318 Yuhangtang Road, Hangzhou, Zhejiang 310000, P.R. China  
E-mail: hzzju@zju.edu.cn

**Key words:** *Astragalus* polysaccharides, pulmonary fibrosis, epithelial-mesenchymal transition, NF- $\kappa$ B pathway

in IPF. The potential roles of certain TCHs in the regulation of IPF remain unexplored. *Astragalus* is a plant that has been used in traditional Chinese medicine for centuries, which is commonly used to treat certain diseases. Numerous studies reported that *Astragalus* could have some immunoregulatory and antitumor effects (10-13). Recent studies demonstrated that *Astragalus* polysaccharides (APS), which are the major components of *Astragalus*, also have some antitumor and anti-fibrotic effects (11,14). However, no study evaluated the role of APS in PF. The present study aimed to explore the potential role and underlying mechanism of APS in IPF. To do so, a bleomycin (BLM)-induced PF mouse model and *in vitro* model of transforming growth factor  $\beta$ 1(TGF- $\beta$ 1)-stimulated human lung epithelial cells were established. Considering the crucial role of NF- $\kappa$ B signaling and TGF- $\beta$ 1 activity in PF, the effect of APS on TGF- $\beta$ 1-induced NF- $\kappa$ B signaling was also assessed. The results from the present study may provide novel insights into the underlying mechanism of APS in PF and allow the development of novel therapeutic options for patients with IPF.

## Materials and methods

**Animal model and cell culture.** The present study was approved by the Institutional Animal Care and Use Committee of Zhejiang University, Hangzhou, China. A total of 30 male C57BL/6 mice (6-8 weeks old) purchased from Vital River Laboratory Animal Technology were used in this study. Mice were anesthetized by intraperitoneal injection of 0.1 ml of sodium pentobarbital at the dose of 50 mg/kg and received 5 mg/kg BLM (Nippon Kayaku Co., Ltd.) or an equal volume of sterile saline by intratracheal administration.

APS was obtained from Shanghai Yuanye Bio-Technology Co., Ltd. and was prepared as described previously (15,16). Mice were treated with either saline or APS (200 mg/kg/day) daily through gavage seven days prior to BLM administration. The day following BLM administration, mice received 200 mg/kg APS daily by gavage until the end of experiment (15). On days 28, six mice per group were anesthetized with sodium pentobarbital (75 mg/kg) prior to cervical dislocation, and lung tissues were collected and immediately frozen in liquid nitrogen for further experiments.

The primary human bronchial epithelial cells and the human lung epithelial cell line A549 were obtained from the Cell Bank of Type Culture Collection of the Chinese Academy of Sciences. Cells were cultured in F-12K Medium supplemented with 10% fetal bovine serum, 100 U/ml penicillin and 100  $\mu$ g/ml streptomycin (all from Gibco; Thermo Fisher Scientific, Inc.) and placed at 37°C in a humidified incubator containing 5% CO<sub>2</sub>. A549 cells was treated with TGF- $\beta$ 1 (10 ng/ml; PeproTech) or 50  $\mu$ mol/l of the NF- $\kappa$ B inhibitor pyrrolidine dithiocarbamate (PDT; cat. no. P8765; Sigma-Aldrich; Merck KGaA) for 24 h. Cells were cultured in medium supplemented with 50 mg/ml APS (Shanghai Yuanye Bio-Technology Co., Ltd.; >98% purity) for 3 days (APS group) (17).

**Hematoxylin and eosin (H&E) staining and Masson's trichrome staining.** Lung tissues from mice were fixed in 4% paraformaldehyde for 24 h at 4°C and embedded in paraffin. Sections

(4-mm thick) were prepared and subsequently stained with H&E and Masson's trichrome for histopathological examination. Images were acquired by an experienced pathologist with an Olympus microscope (magnification,  $\times$ 40). The fibrotic area was quantified using Image Pro Plus 6.0 (Media Cybernetics, Inc.).

**Measurement of hydroxyproline (HYP) content.** The content in matrix proteins in lung tissues was determined by using the Hydroxyproline detection kit (cat. no. A030-3; Nanjing Jiancheng Bioengineering Institute) according to the manufacturer's instructions. The lung tissues were prepared for hydrolysis, adjusting the PH value to 6.0-6.8. Double distilled water was added and tissues were incubated at room temperature for 20 min. Subsequently, the developing solution was added to the tissues that were incubated at 37°C for 5 min. Absorbance was read at 550 nm using a microplate reader. Data were expressed as micrograms ( $\mu$ g) of HYP per mg of dry lung tissue.

**Western blotting, reverse transcription-quantitative (RT-q) PCR and immunofluorescence (IF).** Western blotting, RT-qPCR and IF were performed as described previously (18-20). The primary antibodies for western blotting and IF are provided in Table S1.

Western blotting was performed as described previously (18,19). Proteins were extracted from lung tissues and A549 cells using RIPA lysis buffer at 4°C. Proteins (10  $\mu$ g) were separated by 10% SDS-PAGE and transferred onto polyvinylidene fluoride membranes. Membranes were blocked with 3% BSA in TBST at room temperature for 60 min. Membranes were incubated with primary antibodies overnight at 4°C and with secondary antibody for 1 h at room temperature.  $\beta$ -actin was used as a control and Lamin B1 was used as a nuclear control. Signals were visualized by using an enhanced chemiluminescence detection kit (Auragene Technology, Co., Inc.). Densitometric analysis was performed using Image Pro Plus v 6.0 (Media Cybernetics, Inc.).

RT-qPCR was performed as described previously (18,19). Total RNA was extracted from mice lung samples with TRIzol reagent. The sequences of the primers were as follows: Collagen-1a1, forward 5'-GCCCCGACCCCAAGGAAAAGAAGC-3', reverse 5'-CTGGGAGGCCTCGGTGGACATAG-3'; collagen-3a1, forward 5'-GCCACAGCCTTCTACACCT-3', reverse 5'-GCCAGGGTCACCATTTCTC-3'; fibronectin, forward 5'-GATGTCCGAACAGCTATTTACCA-3', reverse 5'-CCTTGCGACTTCAGCCACT-3'; and GAPDH, forward 5'-TGCACCACCAACTGCTTAGC-3' and reverse 5'-GGCATGGACTGTGGTCATGAG-3'. The relative expression levels were normalized to endogenous control GAPDH and were expressed as 2<sup>- $\Delta\Delta$ C<sub>q</sub></sup> (21) using ABI software v2.3 (Applied Biosystems).

IF was performed as described previously (18,20). Briefly, lung tissues and A549 cells were fixed, permeabilized and incubated for 1 h at 37°C with primary antibody. The appropriate Alexa Fluor linked secondary antibody was applied for 30 min at room temperature. Cells were counterstained with DAPI and images were acquired with a fluorescence microscope.

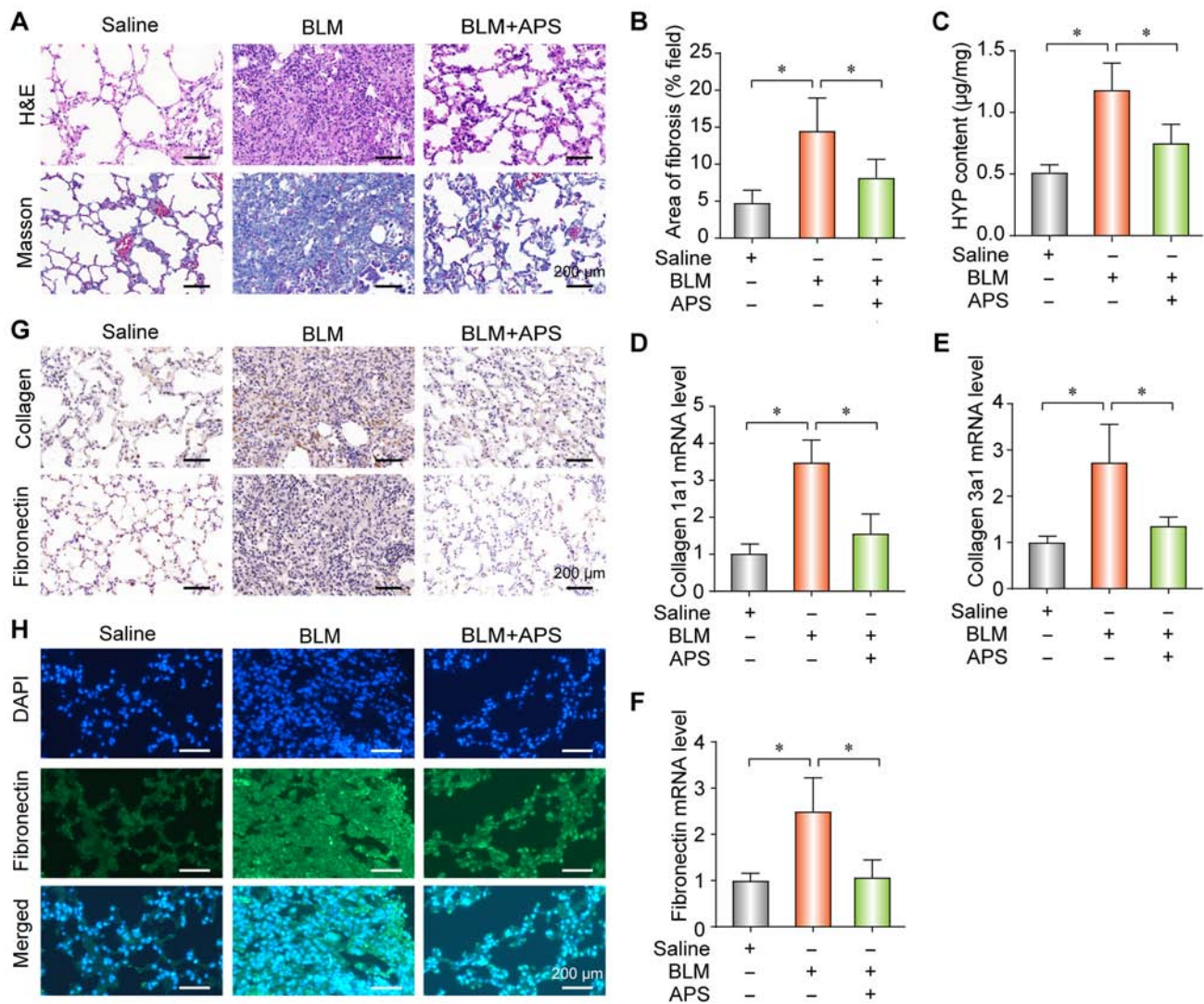


Figure 1. APS attenuated BLM-induced pulmonary fibrosis in mice. (A) Histological images showing collagen deposition in lung tissue from mice treated with saline, BLM, or BLM + APS after hematoxylin and eosin and Masson's stainings. (B and C) Measurement of (B) fibrotic area and (C) HYP content. (D-F) Reverse transcription quantitative PCR analysis of the expression level of (D) collagen 1a1, (E) collagen 3a1 and (F) fibronectin. (G) Immunohistochemical analysis of collagen and fibronectin expression. (H) Immunofluorescence analysis of fibronectin expression. \* $P < 0.05$ . APS, *Astragalus polysaccharides*; BLM, bleomycin; H&E, hematoxylin and eosin; HYP, hydroxyproline. Data are presented as the means  $\pm$  standard deviation.

**Immunohistochemistry (IHC).** IHC and subsequent analyses were performed as described previously (19,20). The primary antibodies used for IHC are presented in Table SI. Briefly, formalin-fixed and paraffin embedded mice lung samples were cut into 5- $\mu$ m-thick sections. Sections were incubated with the primary antibodies at 4°C overnight. Images were acquired on an Olympus microscope. The EnVision kit (Dako; Agilent Technologies, Inc.) was used to detect the signal.

**Ethynyl deoxyuridine (EdU) assay.** A Click-iT Ethynyl deoxyuridine Imaging Kit (cat. no. C10086; Invitrogen; Thermo Fisher Scientific, Inc.) was used for EdU labelling to assess A549 cell proliferation as previously described (18).

**Wound healing assay.** The wound healing assay was performed as described previously (19). A549 cells were cultured in 6-well plates until they reach 100% confluence. The wound was made with a 200  $\mu$ l sterile pipet tip and 1% FBS was added to the medium.

**Statistical analysis.** Statistical analyses were performed using GraphPad Prism software version 5.0 (GraphPad Software, Inc.) and SPSS version 19.0 (IBM Corp.). Unpaired Student's t-test was used for comparison between two groups. One-way ANOVA followed by Student-Newman-Keuls post hoc test was used for comparison between  $\geq 3$  groups. The data were presented as the means  $\pm$  standard deviation of three independent experiments.  $P < 0.05$  was considered to indicate a statistically significant difference.

## Results

**APS reduces BLM-induced PF in mice.** To evaluate the effect of APS on PF, a BLM-induced PF mouse model was established. The establishment of the PF model was verified by H&E staining and Masson's trichrome assay, and the results confirmed the collagen deposition (Fig. S1A) and the increase in fibrotic area (Fig. S1B). Furthermore, the results from RT-qPCR demonstrated that the expression level of

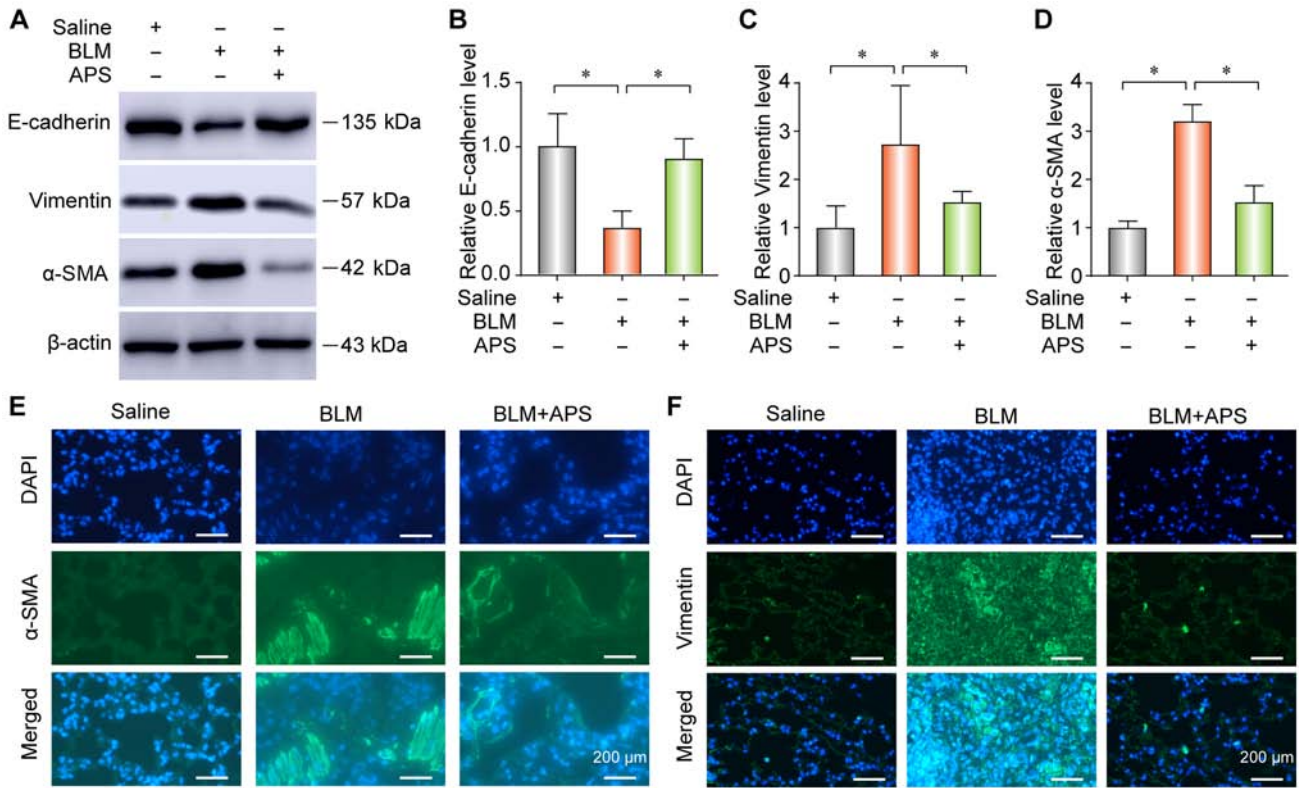


Figure 2. APS suppressed BLM-induced epithelial-mesenchymal transition in pulmonary fibrosis in mice. (A-D) Western blotting analysis and relative quantification levels of E-cadherin, vimentin and  $\alpha$ -SMA expression. (E and F) Immunofluorescence analysis of vimentin and  $\alpha$ -SMA expression. \* $P < 0.05$ .  $\alpha$ -SMA, alpha smooth muscle actin; APS, *Astragalus* polysaccharides; BLM, bleomycin.

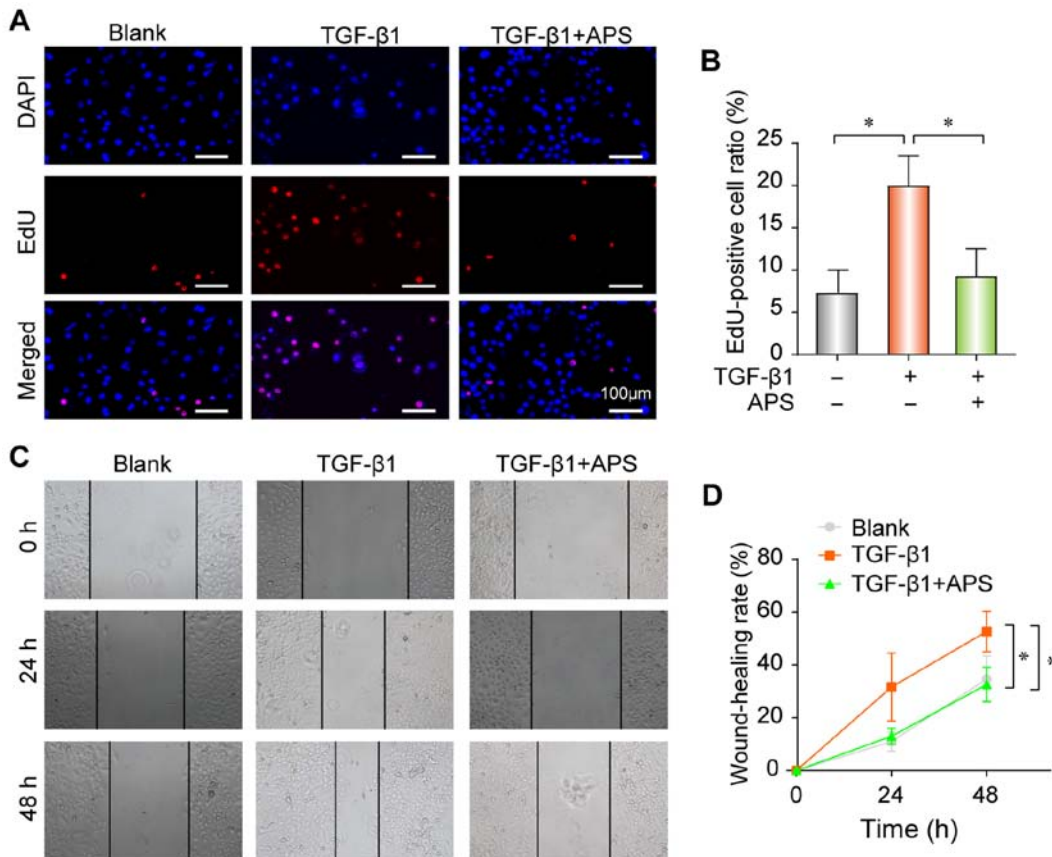


Figure 3. APS alleviated TGF- $\beta$ 1-induced lung fibroblast activation. (A and B) Proliferative capacity analysis via EdU assay. (C and D) Wound healing assay for the assessment of cell migration. APS, *Astragalus* polysaccharides; TGF- $\beta$ 1, transforming growth factor  $\beta$ 1. \* $P < 0.05$ . Data are presented as the means  $\pm$  standard deviation.

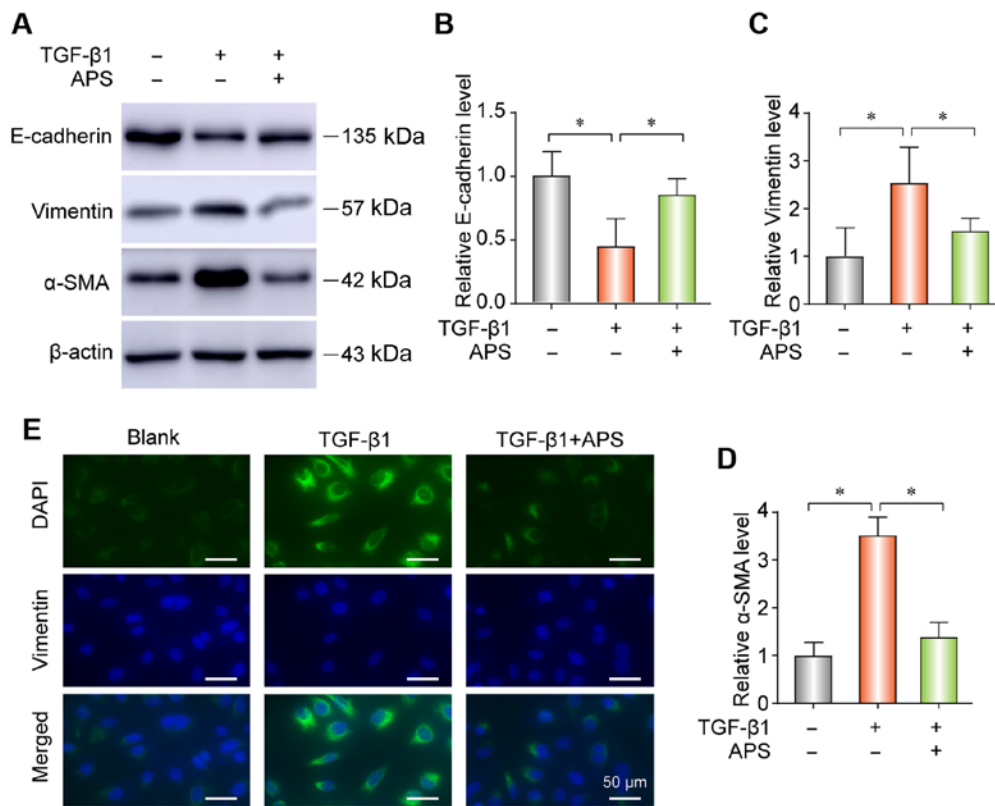


Figure 4. APS inhibited TGF- $\beta$ 1-induced epithelial-mesenchymal transition in pulmonary epithelial cells. (A-D) Western blotting analysis and relative quantification levels of E-cadherin, vimentin and  $\alpha$ -SMA expression. (E) Immunofluorescence analysis of vimentin expression. ( $\alpha$ -SMA, alpha smooth muscle actin; APS, *Astragalus* polysaccharides; TGF- $\beta$ 1, transforming growth factor  $\beta$ 1). \* $P < 0.05$ . Data are presented as the means  $\pm$  standard deviation.

collagen-1a1, collagen-3a1 and fibronectin was increased in lung tissues from BLM-treated mice compared with lung tissues from the saline control group mice (Fig. S1C-E). Furthermore, results from IHC and IF demonstrated an increase in the fibrosis-related proteins collagen and fibronectin in the PF mouse model (Fig. S1F and G). These results confirmed that the BLM-induced PF model was successfully established.

To explore the potential therapeutic effects of APS in PF, APS was administered to the BLM-induced PF mouse model by gavage. The results demonstrated that APS reduced collagen deposition (Fig. 1A), fibrotic area (Fig. 1B) and HYP content (Fig. 1C), which all together are indicators of PF. Furthermore, APS alleviated the BLM-induced up-regulation of collagen-1a1 (Fig. 1D), collagen-3a1 (Fig. 1E) and fibronectin (Fig. 1F) at the mRNA level. In addition, the results from IHC and IF demonstrated that APS inhibited the BLM-induced upregulation of collagen and fibronectin (Fig. 1G and 1H, respectively). These findings suggested that APS may attenuate BLM-induced PF.

**APS inhibits BLM-induced EMT in mice with PF.** To explore the occurrence of EMT during PF, the expression of the epithelial marker E-cadherin and of the mesenchymal markers vimentin and alpha smooth muscle actin ( $\alpha$ -SMA) were determined by western blotting or IF. The results from western blotting (Fig. 2A-D) and IF (Fig. 2E and F) demonstrated that BLM treatment significantly reduced E-cadherin expression and upregulated the expression of vimentin and  $\alpha$ -SMA in lung tissues. These data suggested that epithelial cells decreased

and myofibroblasts increased during PF. However, the results from western blotting and IF demonstrated that treatment with APS could reverse BLM-induced EMT, along with a decrease in vimentin and  $\alpha$ -SMA expression and an increase in the E-cadherin expression (Fig. 2A-D, E and F).

**APS decreases TGF- $\beta$ 1-induced fibrogenesis in pulmonary epithelial cells.** The proliferation and differentiation of fibroblasts serve crucial roles in PF, and can promote extracellular matrix (ECM) deposition and aggravate therefore fibrosis. The results from the present study demonstrated that TGF- $\beta$ 1 promoted the proliferation (Fig. 3A and B) and migratory ability (Fig. 3C and D) of pulmonary epithelial cells *in vitro*, whereas these effects were nearly completely reversed following treatment with APS. EMT is commonly known to be induced by TGF- $\beta$ 1 (22,23). The results from western blotting indicated that TGF- $\beta$ 1 could upregulate the expression of  $\alpha$ -SMA and vimentin and reduce the expression of E-cadherin in A549 cells (Fig. 4A-D). However, cell treatment with APS reversed these changes. The results from IF demonstrated that TGF- $\beta$ 1 could increase vimentin expression in A549 cells (Fig. 4E).

**APS inhibits TGF- $\beta$ 1-induced NF- $\kappa$ B pathway activation in pulmonary epithelial cells.** Considering the essential role of TGF- $\beta$ 1 activity and NF- $\kappa$ B signaling in PF, the effect of APS on TGF- $\beta$ 1-induced NF- $\kappa$ B signaling was evaluated in the present study. Cell treatment with TGF- $\beta$ 1 increased the nuclear translocation of p65 (Fig. 5A and B) and the

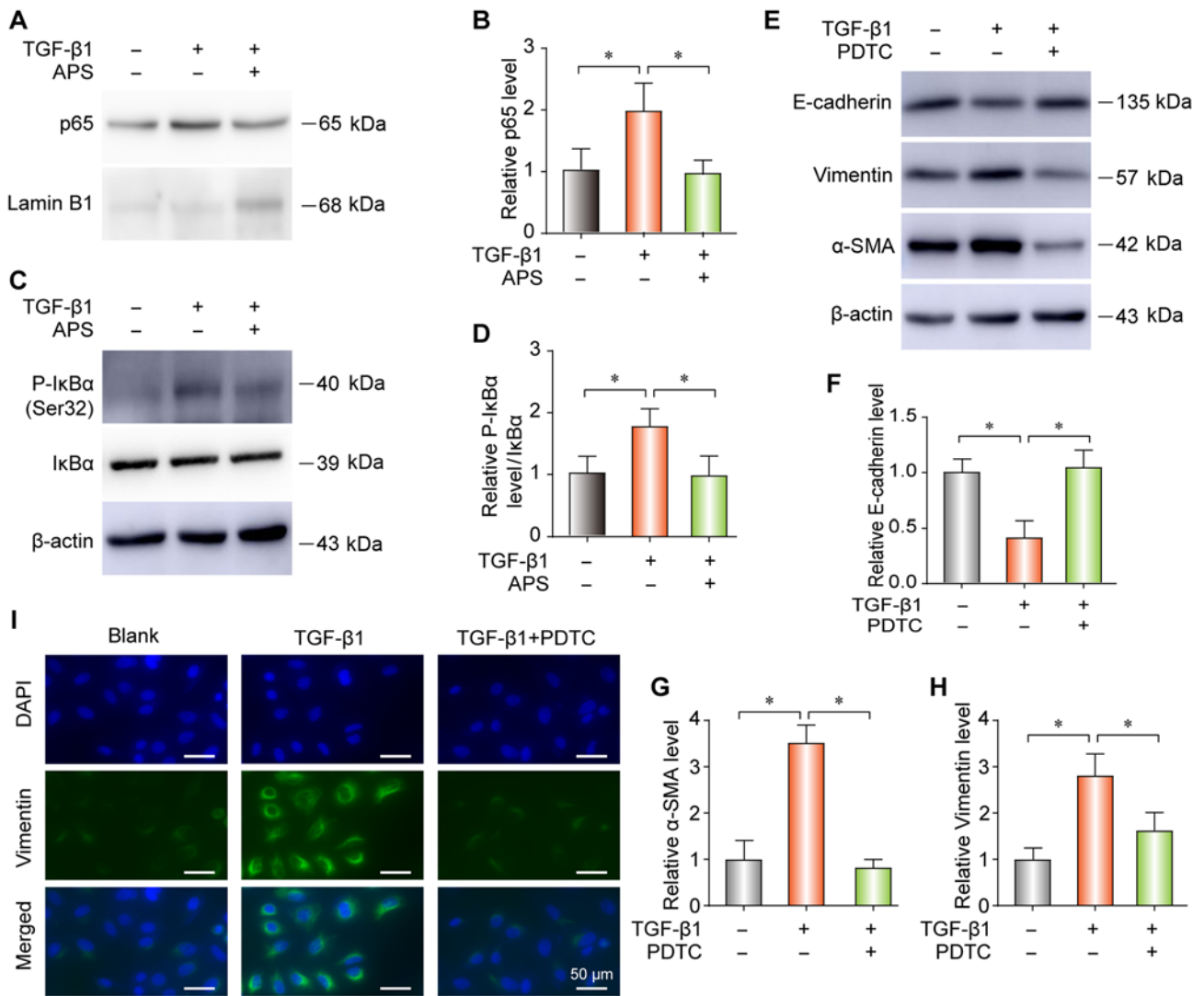


Figure 5. APS and PDTC decreased TGF-β1-induced NF-κB pathway activation in pulmonary epithelial cells. (A-D) Western blotting analysis and relative quantification levels of p65 and P-IκBα expression following APS and TGF-β1 treatment. (E-H) Western blotting analysis and relative quantification levels of E-cadherin, vimentin and α-SMA expression following PDTC and TGF-β1 treatment. (I) Immunofluorescence analysis of vimentin expression following PDTC and TGF-β1 treatment. (α-SMA, alpha smooth muscle actin; APS, *Astragalus* polysaccharides; P, phospho; PDTC, pyrrolidine dithiocarbamate; TGF-β1, transforming growth factor β1. \*P<0.05. Data are presented as the means ± standard deviation.

expression level of phospho (p-) IκBα (Fig. 5C and D). Furthermore, APS blocked the NF-κB pathway activation by TGF-β1 (Fig. 5A-D). In addition, PDTC (24) neutralized the TGF-β1-induced increase in E-Cadherin, vimentin and α-SMA expression by western blot (Fig. 5E-H) or IF (Fig. 5I). Furthermore, TGF-β1 increased the proliferation (Fig. 6A and B) and migratory ability (Fig. 6C and D) of pulmonary epithelial cells; however, these effects were reversed following treatment with PDTC. Taken together, these findings indicate that the NF-κB signaling pathway may serve a crucial role in TGF-β1-induced EMT in A549 cells, and that TGF-β1-induced PF progression may be inhibited by APS via the NF-κB pathway.

**Discussion**

EMT serves a key role in the occurrence and development of PF. During EMT, the expression in epithelial cells of adherens junction proteins, including E-cadherin, is

decreased whereas the expression of fibroblast markers, including vimentin and α-SMA, is increased (25,26). One of the histological characteristics of PF is the ECM deposition. The cytokine TGF-β1 is an important regulator of fibrogenesis. TGF-β1 activates fibroblasts and transforms them into myofibroblasts (2,3). Numerous studies reported that TGF-β1 is a key fibrogenic factor, which can induce EMT in PF (27). Subsequently, inhibition of EMT through the TGF-β1 pathway may be considered as a potential therapeutic option for IPF.

Previous studies reported the antitumor (28), anti-diabetic (29), antioxidant and immunomodulatory properties of APS (30,31). Several studies demonstrated that *Astragalus* has strong anti-fibrotic activities (12,15). *Astragalus* was found to inhibit the EMT of peritoneal mesothelial cells by decreasing β-catenin expression (32). Furthermore, it was reported that *Astragalus* has some therapeutic effects on BLM-induced PF by reducing Jagged1/Notch1 expression (33). Furthermore, *Astragalus* saponins could reduce liver fibrosis

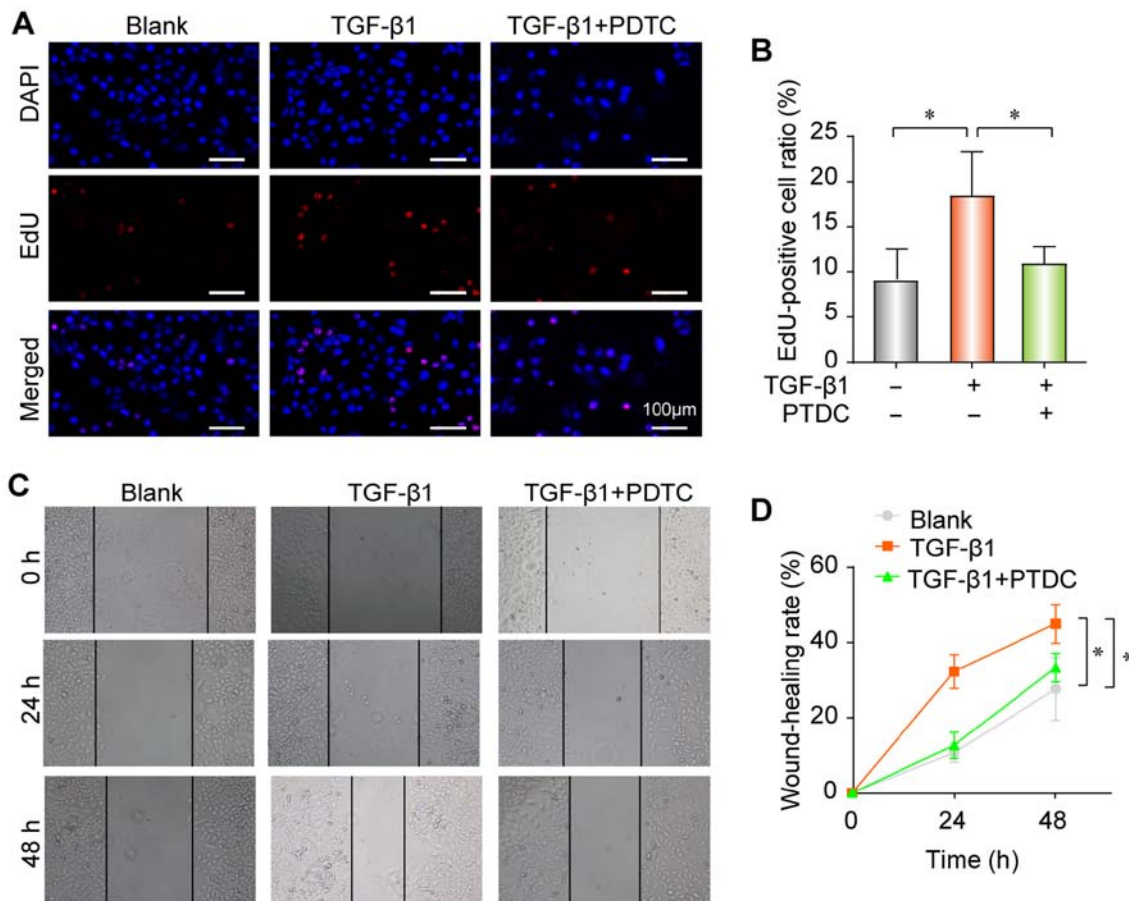


Figure 6. PDTC alleviated TGF- $\beta$ 1-induced lung fibroblast activation. (A and B) Proliferative capacity evaluated by the EdU assay. (C and D) Wound-healing assay to examine cell migration. (PDTC, pyrrolidine dithiocarbamate; TGF- $\beta$ 1, transforming growth factor  $\beta$ 1. \* $P$ <0.05. Data are presented as the means  $\pm$  standard deviation.

by decreasing TGF- $\beta$ 1/Smad signaling pathway (34). Astragaloside IV isolated from *Astragalus* can reduce the hyperphosphorylation of forkhead box O3a induced by TGF- $\beta$ 1/PI3K/Akt and reverse EMT involved in the process of fibrosis (35). In the present study, APS attenuated BLM-induced PF and EMT in mice. These results were similar to those from a previous study demonstrating that APS can inhibit excessive collagen accumulation in a BLM-induced scleroderma mouse model (36).

Toll-like receptor 4 (TLR4)/NF- $\kappa$ B pathway activation is a key mechanism involved in the inflammatory response observed in pulmonary disease (37,38). NF- $\kappa$ B signaling is activated by TLR4 via the stimulation of released inflammatory cytokines, which promote the proinflammatory response. Under normal conditions, NF- $\kappa$ B is isolated in the cytoplasm and binds to I $\kappa$ B. Once activated, NF- $\kappa$ B translocates to the nucleus and regulates the production of inflammatory cytokines (39,40).

In the present study, treatment with PDTC alleviated PF in BLM-treated mice. These findings suggested that NF- $\kappa$ B may serve an important role in the progression of PF, which may be reversed by inhibiting NF- $\kappa$ B signaling. A previous study reported that APS reduces inflammation by inhibiting the activation of the TLR-4/NF- $\kappa$ B pathway and protects mice from coxsackievirus B3-induced viral myocarditis (15). In the present study, APS attenuated BLM-induced PF and EMT in

mice. Furthermore, APS reduced the TGF- $\beta$ 1-induced EMT and NF- $\kappa$ B pathway activation in pulmonary epithelial cells. Taken together, these findings suggested that APS may have an anti-fibrotic effect by repressing the activation of the NF- $\kappa$ B signaling pathway, preventing therefore EMT progression and ameliorating PF.

In conclusion, the present study demonstrated that APS could alleviate PF *in vitro* and *in vivo* and reduce the TGF- $\beta$ 1-induced NF- $\kappa$ B pathway activation. To the best of our knowledge, this study was the first to demonstrate the APS-mediated alleviation of PF *in vitro* and *in vivo*. In addition, this study elucidated some mechanism of action of APS in PF, suggesting that APS may be considered as a therapeutic agent to treat IPF.

#### Acknowledgements

Not applicable.

#### Funding

This study was supported by the Zhejiang Provincial Natural Science Foundation of China (grant nos. LY19H160057 to SL, LY19H030013 to RM and LY15H030011 to LZ.), the Zhejiang Provincial Public Welfare Technology Research Plan of China (grant no. LGD19H030003 to XA) and the Chinese

Medicine Science and Technology Plan of Zhejiang Province (grant no. 2019ZA070 to XA).

### Availability of data and materials

The analyzed datasets generated during the study are available from the corresponding author on reasonable request.

### Authors' contributions

SL, XS and XA designed the study. RZ performed all experiments. LX analyzed the data. SL and XS wrote the article. All authors discussed the results and revised the article. All authors read and approved the final manuscript.

### Ethics approval and consent to participate

This study was approved by The Institutional Research Board of the First Affiliated Hospital, College of Medicine, Zhejiang University.

### Patient consent for publication

Not applicable.

### Competing interests

The authors declare that they have no competing interests.

### References

- Lederer DJ and Martinez FJ: Idiopathic pulmonary fibrosis. *N Engl J Med* 378: 797-798, 2018.
- Richeldi L, Collard HR and Jones MG: Idiopathic pulmonary fibrosis. *Lancet* 389: 1941-1952, 2017.
- Hutchinson J, Fogarty A, Hubbard R and McKeever T: Global incidence and mortality of idiopathic pulmonary fibrosis: A systematic review. *Eur Respir J* 46: 795-806, 2015.
- Wolters PJ, Collard HR and Jones KD: Pathogenesis of idiopathic pulmonary fibrosis. *Annu Rev Pathol* 9: 157-179, 2014.
- Raghu G: Idiopathic pulmonary fibrosis: Combating on a new turf. *Lancet Respir Med* 4: 430-432, 2016.
- Liu YM, Nepali K and Liou JP: Idiopathic pulmonary fibrosis: Current status, recent progress, and emerging targets. *J Med Chem* 60: 527-553, 2017.
- Vancheri C, Kreuter M, Richeldi L, Ryerson CJ, Valeyre D, Grutters JC, Wiebe S, Stansen W, Quaresima M, Stowasser S, *et al*: Nintedanib with add-on pirfenidone in idiopathic pulmonary fibrosis. Results of the INJOURNEY trial. *Am J Respir Crit Care Med* 197: 356-363, 2018.
- Wang R, Sun Q, Wang F, Liu Y, Li X, Chen T, Wu X, Tang H, Zhou M, Zhang S, *et al*: Efficacy and safety of chinese herbal medicine on ovarian cancer after reduction surgery and adjuvant chemotherapy: A systematic review and meta-analysis. *Front Oncol* 9: 730, 2019.
- Zhai B, Zhang N, Han X, Li Q, Zhang M, Chen X, Li G, Zhang R, Chen P, Wang W, *et al*: Molecular targets of  $\beta$ -elemene, a herbal extract used in traditional Chinese medicine, and its potential role in cancer therapy: A review. *Biomed Pharmacother* 114: 108812, 2019.
- Lin S, An X, Guo Y, Gu J, Xie T, Wu Q and Sui X: Meta-analysis of *Astragalus*-containing traditional chinese medicine combined with chemotherapy for colorectal cancer: Efficacy and safety to tumor response. *Front Oncol* 9: 749, 2019.
- Liu C, Li H, Wang K, Zhuang J, Chu F, Gao C, Liu L, Feng F, Zhou C, Zhang W and Sun C: Identifying the antiproliferative effect of *Astragalus* polysaccharides on breast cancer: Coupling network pharmacology with targetable screening from the cancer genome atlas. *Front Oncol* 9: 368, 2019.
- Huang KC, Su YC, Sun MF and Huang ST: Chinese herbal medicine improves the long-term survival rate of patients with chronic kidney disease in taiwan: A nationwide retrospective population-based cohort study. *Front Pharmacol* 9: 1117, 2018.
- Chen X, Chen X, Gao J, Yang H, Duan Y, Feng Y, He X, Gong X, Wang H, Wu X and Chang J: Astragaloside III enhances anti-tumor response of NK cells by elevating NKG2D and IFN- $\gamma$ . *Front Pharmacol* 10: 898, 2019.
- Ren L, Guo XY, Gao F, Jin ML and Song XN: Identification of the perturbed metabolic pathways associating with renal fibrosis and evaluating metabolome changes of pretreatment with astragalus polysaccharide through liquid chromatography quadrupole time-of-flight mass spectrometry. *Front Pharmacol* 10: 1623, 2020.
- Liu T, Zhang M, Niu H, Liu J, Ruilian M, Wang Y, Xiao Y, Xiao Z, Sun J, Dong Y and Liu X: *Astragalus* polysaccharide from *Astragalus* Melittin ameliorates inflammation via suppressing the activation of TLR-4/NF- $\kappa$ B p65 signal pathway and protects mice from CVB3-induced virus myocarditis. *Int J Biol Macromol* 126: 179-186, 2019.
- Li XT, Zhang YK, Kuang HX, Jin FX, Liu DW, Gao MB, Liu Z and Xin XJ: Mitochondrial protection and anti-aging activity of *Astragalus* polysaccharides and their potential mechanism. *Int J Mol Sci* 13: 1747-1761, 2012.
- Zhang L, Luo Y, Lu Z, He J, Wang L, Zhang L, Zhang Y and Liu Y: *Astragalus* polysaccharide inhibits ionizing radiation-induced bystander effects by regulating MAPK/NF- $\kappa$ B signaling pathway in bone mesenchymal stem cells (BMSCs). *Med Sci Monit* 24: 4649-4658, 2018.
- Lin S, Zhang R, An X, Li Z, Fang C, Pan B, Chen W, Xu G and Han W: LncRNA HOXA-AS3 confers cisplatin resistance by interacting with HOXA3 in non-small-cell lung carcinoma cells. *Oncogenesis* 8: 60, 2019.
- Lin S, Zhou S, Jiang S, Liu X, Wang Y, Zheng X, Zhou H, Li X and Cai X: NEK2 regulates stem-like properties and predicts poor prognosis in hepatocellular carcinoma. *Oncol Rep* 36: 853-862, 2016.
- Zhai S, Lin S, Lin Z, Xu J, Ji T, Chen K, Wu K, Liu H, Ying H, Fei W, *et al*: eIF4EBP3 was downregulated by methylation and acted as a tumor suppressor by targeting eIF4E/ $\beta$ -catenin in gastric cancer. *Gastric Cancer* 2019 (Epub ahead of print).
- Livak KJ and Schmittgen TD: Analysis of relative gene expression data using real-time quantitative PCR and the 2<sup>-</sup>(Delta Delta C(T)) method. *Methods* 25: 402-408, 2001.
- Zheng Q, Tong M, Ou B, Liu C, Hu C and Yang Y: Isorhamnetin protects against bleomycin-induced pulmonary fibrosis by inhibiting endoplasmic reticulum stress and epithelial-mesenchymal transition. *Int J Mol Med* 43: 117-126, 2019.
- Zhu X, Li Q, Hu G, Wang J, Hu Q, Liu Z, Wu G and Zhong Y: BMS-345541 inhibits airway inflammation and epithelial-mesenchymal transition in airway remodeling of asthmatic mice. *Int J Mol Med* 42: 1998-2008, 2018.
- Liu F, Zhang X, Zhang B, Mao W, Liu T, Sun M and Wu Y: TREM1: A positive regulator for inflammatory response via NF- $\kappa$ B pathway in A549 cells infected with mycoplasma pneumoniae. *Biomed Pharmacother* 107: 1466-1472, 2018.
- Lin HY, Liang YK, Dou XW, Chen CF, Wei XL, De Zeng, Bai JW, Guo YX, Lin FF, Huang WH, *et al*: Notch3 inhibits epithelial-mesenchymal transition in breast cancer via a novel mechanism, upregulation of GATA-3 expression. *Oncogenesis* 7: 59, 2018.
- Li N, Babaei-Jadidi R, Lorenzi F, Spencer-Dene B, Clarke P, Domingo E, Tulchinsky E, Vries RGJ, Kerr D, Pan Y, *et al*: An FBXW7-ZEB2 axis links EMT and tumour microenvironment to promote colorectal cancer stem cells and chemoresistance. *Oncogenesis* 8: 13, 2019.
- Zhu HF, Liu YP, Liu DL, Ma YD, Hu ZY, Wang XY, Gu CS, Zhong Y, Long T, Kan HP and Li ZG: Role of TGF $\beta$ 3-Smads-Spl axis in DcR3-mediated immune escape of hepatocellular carcinoma. *Oncogenesis* 8: 43, 2019.
- Bao WR, Li ZP, Zhang QW, Li LF, Liu HB, Ma DL, Leung CH, Lu AP, Bian ZX and Han QB: *Astragalus* polysaccharide RAP selectively attenuates paclitaxel-induced cytotoxicity toward RAW 264.7 cells by reversing cell cycle arrest and apoptosis. *Front Pharmacol* 9: 1580, 2019.
- Liu P, Peng QH, Tong P and Li WJ: *Astragalus* polysaccharides suppresses high glucose-induced metabolic memory in retinal pigment epithelial cells through inhibiting mitochondrial dysfunction-induced apoptosis by regulating miR-195. *Mol Med* 25: 21, 2019.

30. Jia N, Qiao H, Zhu W, Zhu M, Meng Q, Lu Q and Zu Y: Antioxidant, immunomodulatory, oxidative stress inhibitory and iron supplementation effect of *Astragalus membranaceus* polysaccharide-iron (III) complex on iron-deficiency anemia mouse model. *Int J Biol Macromol* 132: 213-221, 2019.
31. Jin M, Zhao K, Huang Q and Shang P: Structural features and biological activities of the polysaccharides from *Astragalus membranaceus*. *Int J Biol Macromol* 64: 257-266, 2014.
32. Yu M, Shi J, Sheng M, Gao K, Zhang L, Liu L and Zhu Y: *Astragalus* inhibits epithelial-to-mesenchymal transition of peritoneal mesothelial cells by down-regulating  $\beta$ -catenin. *Cell Physiol Biochem* 51: 2794-2813, 2018.
33. Zhou Y, Liao S, Zhang Z, Wang B and Wan L: *Astragalus* injection attenuates bleomycin-induced pulmonary fibrosis via down-regulating Jagged1/Notch1 in lungs. *J Pharm Pharmacol* 68: 389-396, 2016.
34. Zhou Y, Tong X, Ren S, Wang X, Chen J, Mu Y, Sun M, Chen G, Zhang H and Liu P: Synergistic anti-liver fibrosis actions of total *Astragalus* saponins and glycyrrhizic acid via TGF- $\beta$ 1/Smads signaling pathway modulation. *J Ethnopharmacol* 190: 83-90, 2016.
35. Qian W, Cai X, Qian Q, Zhang W and Wang D: Astragaloside IV modulates TGF- $\beta$ 1-dependent epithelial-mesenchymal transition in bleomycin-induced pulmonary fibrosis. *J Cell Mol Med* 22: 4354-4365, 2018.
36. Hao ZF, Su YM, Liu JY, Wang CM and Yang RY: *Astragalus* polysaccharide suppresses excessive collagen accumulation in a murine model of bleomycin-induced scleroderma. *Int J Clin Exp Med* 8: 3848-3854, 2015.
37. Tian Y, Li H, Qiu T, Dai J, Zhang Y, Chen J and Cai H: Loss of PTEN induces lung fibrosis via alveolar epithelial cell senescence depending on NF- $\kappa$ B activation. *Aging Cell* 18: e12858, 2019.
38. Chae U, Lee H, Kim B, Jung H, Kim BM, Lee AH, Lee DS and Min SH: A negative feedback loop between XBP1 and Fbw7 regulates cancer development. *Oncogenesis* 8: 12, 2019.
39. Tian B, Zhao Y, Sun H, Zhang Y, Yang J and Brasier AR: BRD4 mediates NF- $\kappa$ B-dependent epithelial-mesenchymal transition and pulmonary fibrosis via transcriptional elongation. *Am J Physiol Lung Cell Mol Physiol* 311: L1183-L1201, 2016.
40. Ishak Gabra MB, Yang Y, Lowman XH, Reid MA, Tran TQ and Kong M: IKK $\beta$  activates p53 to promote cancer cell adaptation to glutamine deprivation. *Oncogenesis* 7: 93, 2018.



This work is licensed under a Creative Commons Attribution-NonCommercial-NoDerivatives 4.0 International (CC BY-NC-ND 4.0) License.